

# Role of Interleukin-1 in Radiation-Induced Cardiomyopathy

Eleonora Mezzaroma,<sup>1,2,3</sup> Ross B Mikkelsen,<sup>4</sup> Stefano Toldo,<sup>1,2</sup> Adolfo G Mauro,<sup>1,2</sup> Khushboo Sharma,<sup>5</sup> Carlo Marchetti,<sup>1,2</sup> Asim Alam,<sup>4</sup> Benjamin W Van Tassell,<sup>1,2,3</sup> David A Gewirtz,<sup>5</sup> and Antonio Abbate<sup>1,2</sup>

<sup>1</sup>Virginia Commonwealth University (VCU) Pauley Heart Center, Richmond, Virginia, United States of America; <sup>2</sup>VCU Victoria Johnson Center, Richmond, Virginia, United States of America; <sup>3</sup>School of Pharmacy, VCU, Richmond, Virginia, United States of America; <sup>4</sup>Radiation Oncology, Massey Cancer Center, VCU, Richmond, Virginia, United States of America; and <sup>5</sup>Pharmacology and Toxicology, Massey Cancer Center, VCU, Richmond, Virginia, United States of America

Thoracic X-ray therapy (XRT), used in cancer treatment, is associated with increased risk of heart failure. XRT-mediated injury to the heart induces an inflammatory response leading to cardiomyopathy. The aim of this study was to determine the role of interleukin (IL)-1 in response to XRT injury to the heart and on the cardiomyopathy development in the mouse. Female mice with genetic deletion of the IL-1 receptor type I (IL-1R1 knockout mice (IL-1R1 KO)) and treatment with recombinant human IL-1 receptor antagonist anakinra, 10 mg/kg twice daily for 7 d, were used as independent approaches to determine the role of IL-1. Wild-type (wt) or IL-1R1 KO mice were treated with a single session of XRT (20 or 14 gray (Gy)). Echocardiography (before and after isoproterenol challenge) and left ventricular (LV) catheterization were performed to evaluate changes in LV dimensions and function. Masson's trichrome was used to assess myocardial fibrosis and pericardial thickening. After 20 Gy, the contractile reserve was impaired in wt mice at d 3, and the LV ejection fraction (EF) was reduced after 4 months when compared with sham-XRT. IL-1R1 KO mice had preserved contractile reserve at 3 d and 4 months and LVEF at 4 months after XRT. Anakinra treatment for 1 d before and 7 d after XRT prevented the impairment in contractile reserve. A significant increase in LV end-diastolic pressure, associated with increased myocardial interstitial fibrosis and pericardial thickening, was observed in wt mice, as well as in IL-1R1 KO- or anakinra-treated mice. In conclusion, induction of IL-1 by XRT mediates the development of some, such as the contractile impairment, but not all aspects of the XRT-induced cardiomyopathy, such as myocardial fibrosis or pericardial thickening.

Online address: <http://www.molmed.org>

doi: 10.2119/molmed.2014.00243

## INTRODUCTION

Thoracic X-ray therapy (XRT) is a common treatment in the management of many malignancies. When the field of XRT involves the heart, injury can result at several levels (1,2). The pericardium, myocardium, conduction system, valves and coronary arteries are subject to damage, leading to a heterogeneous clinical syndrome (1,2).

The development of more precisely targeted radiation techniques has reduced total radiation dose and volume of healthy tissues irradiated (1,2). However,

there are still a large number of patients with breast or lung cancer or mediastinal lymphoma who have received significant radiation to the heart in the past or will continue to receive such radiation exposure in the future; as such, they are at risk of developing heart disease (1,2).

XRT-induced cardiomyopathy can present acutely or remain latent, becoming evident only years later (1,2). The effects of XRT are more frequently related to the development of a form of restrictive cardiomyopathy with a mild reduction in left ventricular (LV) systolic function and

more pronounced diastolic dysfunction rather than to a dilated cardiomyopathy with severe LV systolic dysfunction (3).

In recent years, the development of murine models has represented a significant step forward in the understanding of the pathophysiology of XRT-induced cardiomyopathy (4–6). In rodents, a latent phase after XRT in which the animals show a preserved cardiac function and impaired contractile reserve is followed by a late, chronic phase in which there is progression of systolic dysfunction associated with a worsening in the contractile reserve and premature death (4).

XRT activates inflammatory pathways in several cell types, including endothelial cells, macrophages and fibroblasts, that potentially participate in the initiation and amplification of cardiac toxicity (7–10). Interleukin (IL)-1 is the prototypical inflammatory cytokine activated in response to tissue injury (11–13) and has been found to be increased in the heart

---

Address correspondence to Eleonora Mezzaroma, Virginia Commonwealth University, 410 North 12th Street, Box 980533, Richmond, VA 23298. Phone: 804-828-0513; Fax: 360-323-1204; E-mail: [emezzaroma@vcu.edu](mailto:emezzaroma@vcu.edu).

Submitted December 4, 2014; Accepted for publication March 25, 2015; Published Online ([www.molmed.org](http://www.molmed.org)) March 26, 2015.

The Feinstein Institute  
for Medical Research 

Empowering Imagination. Pioneering Discovery.®

and lungs after exposure to ionizing radiation (14,15).

The binding of IL-1 to the type I receptor (IL-1R1) induces the synthesis of a large number of secondary mediators, largely amplifying the inflammatory response and promoting further injury (11). The role of inflammation and IL-1 in the initial damage and progression of XRT-induced cardiomyopathy has not yet been elucidated.

In experimental animal models, IL-1 induces systolic and diastolic dysfunction (16,17). IL-1 blockade with anakinra, a recombinant human IL-1 receptor antagonist (IL-1Ra), provides cardioprotection and improves LV remodeling and function after acute myocardial infarction or doxorubicin-induced injury (18,19).

Herein, we present the results of an investigation into the role of IL-1 in the disease progression in an animal model of XRT-induced cardiomyopathy (4) by using mice lacking the IL-1 signaling (IL-1R1 knockout mice [IL-1R1 KO]) and IL-1 pharmacological blockade with anakinra.

## MATERIALS AND METHODS

### Animals

Female C57BL/6J wild-type (wt) and IL-1R1 KO mice were purchased from The Jackson Laboratory (Bar Harbor, ME, USA) and then bred in the Virginia Commonwealth University animal facility. The IL-1R1 KO mice have a normal phenotype at birth and normal development (20). The mice were housed under conditions of 12-h dark/light cycles and had access to water and food *ad libitum*.

### Irradiation Protocol

Irradiation of organs with limited regeneration capacity results in cumulative damage; therefore, in this study, we chose to use a simple protocol of a single radiation dose to be able to time the events starting from a specific time point. The mice, under light anesthesia (pentobarbital 30–50 mg/kg; Sigma-Aldrich, St. Louis, MO, USA), were irradiated using two different radiation doses, 14 or 20 gray (Gy), to explore a potential dose-

response relationship. Cone beam computed tomography (360 two-dimensional images at 65 kV, 1 mA) was performed by using the small animal radiation research platform (SARRP) (Gulmay Medical, Suwanee, GA, USA) to establish the treatment field. The contrast between the heart, lungs and surrounding tissues was reconstructed with the 3D Slicer software (www.slicer.org), allowing the selection of the isocenter at the heart and the treatment plan. The dose (14 or 20 Gy), calculated with the 3D Slicer software, was delivered as a static vertical beam by using a 1.5-cm diameter circular field with the tube energized to 220 kV, 13.0 mA. After XRT, mice were injected subcutaneously with 0.5 mL saline solution (0.9% NaCl) to avoid dehydration. Body weight was monitored every 3 d after XRT. The irradiated wt and IL-1R1 KO mice were followed for up to 6 months after 14 Gy irradiation. Significant mortality is observed at 4 months after a radiation exposure of 20 Gy (4). For this reason, the studies with 20 Gy were terminated at 4 months. Age-matched sham-irradiated mice were used as the control group. All animal experiments were conducted under the guidelines on humane use and care of laboratory animals for biomedical research (21). The study was approved by the Institutional Animal Care and Use Committee at the Virginia Commonwealth University.

### Anakinra Treatments

Irradiated wt mice were injected intraperitoneally with anakinra, recombinant human IL-1Ra, 10 mg/kg (Swedish Orphan Biovitrum, Stockholm, Sweden) or an equal volume (0.2 mL) of saline. Mice were treated with anakinra every 12 h (to guarantee sustained levels of the drug over 24 h) for 7 d, starting 24 h before XRT treatment, with 20 or 14 Gy.

### Experimental Groups

The following groups were included in the study:

- (a) sham-wt (wt control), n = 8;
- (b) 20Gy-wt, receiving a single dose of radiation of 20 Gy, n = 6–12/group;

- (c) sham-IL-1R1 KO, n = 7;
- (d) 20Gy-IL-1R1 KO, receiving a single dose of radiation of 20 Gy, n = 6–21/group;
- (e) 20Gy-wt+anakinra, receiving 20 Gy and anakinra, n = 5–10/group;
- (f) 14Gy-wt, receiving a single dose of radiation of 14 Gy, n = 8–11/group;
- (g) 14Gy-IL-1R1 KO, receiving a single dose of radiation of 14 Gy n = 10–12/group; and
- (h) 14Gy-wt+anakinra, receiving 14 Gy and anakinra, n = 12–17/group.

### Echocardiography

Transthoracic echocardiography under light anesthesia (pentobarbital 30–50 mg/kg) was performed at baseline, 3 d and 4 months by using the Vevo 770 imaging system (VisualSonic, Toronto, Ontario, Canada) equipped with a 30-MHz probe as previously described (18), according to the American Society of Echocardiography recommendations (22). At each time point, we measured the LV end diastolic diameter (EDD), the LV end systolic diameter (ESD) and the LV ejection fraction (EF) (estimated by using the Teicholz formula). To assess the contractile reserve, mice were injected with 10 ng/mouse isoproterenol, a  $\beta$ -adrenergic receptor agonist (Sigma-Aldrich), as previously described (4). The contractile reserve was calculated as percentage change in LV ejection fraction (LVEF) measured 3 min after isoproterenol injection (LVEFi) and compared with rest (LVEFr) and calculated as [(LVEFi – LVEFr)/LVEFr]  $\times$  100.

### LV Catheterization

To measure the LV pressures, mice were deeply sedated (pentobarbital, 50–70 mg/kg) and a pressure probe catheter (Millar Instruments, Houston, TX, USA) was retrogradely inserted in the left ventricle through the left carotid artery. We measured LV end-diastolic pressure (LVEDP) and  $-dP/dt$ , markers of LV diastolic dysfunction, and the LV peak pressure (LVPSF) and the  $+dP/dt$ , markers of LV systolic function, in sham and XRT-treated mice at 4 months (20 Gy)

and 6 months (14 Gy). The measurements were recorded and analyzed with the Labchart Pro software (Millar Instruments). After the procedure, the mice were sacrificed with an overdose of anesthetic and the hearts were collected for additional studies.

### Assessment of Myocardial and Pericardial Fibrosis

Hearts from mice sacrificed at 4 months (20 Gy) and 6 months (14 Gy) were collected in 10% formalin and then embedded in paraffin as previously described (23). The 5- $\mu\text{m}$ -thick heart slides were stained with Masson trichrome (Thermo Fisher Scientific, Waltham, MA, USA) as instructed by the manufacturer to assess total collagen deposition and pericardium thickness. ImageJ software (<http://rsb.info.nih.gov/ij/>; NIH, Bethesda, MD, USA) was used to quantify the total collagen on total area per field (expressed as percent collagen on total area). Perivascular fibrosis was excluded from this count. Image Pro Plus 6.0 software (Media Cybernetics, Rockville, MD, USA) was used to measure the pericardial thickness, expressed as percent change compared with sham-irradiated mice.

### Capillary Density

Immunohistochemistry was used to quantify capillary density on heart tissue slides by using an antibody raised against caveolin-1 (Cell Signaling Technology, Danvers, MA, USA). Staining with Novared (Vector Laboratories, Burlingame, CA, USA) was used to detect caveolin-1-positive endothelial cells. Capillary density was assessed counting the number of capillaries positive for caveolin-1 per field (40 $\times$  magnification). The measurements were acquired by two investigators blinded to the treatment allocation.

### Statistical Analysis

Statistical analysis was performed by using SPSS 15.0. Continuous variables were expressed as mean and standard error. Two-way analysis of variance was used to compare treated and control val-

ues between two or more groups by using the time-group interaction. A *t* test for unpaired data was used to compare two groups, and one-way analysis of variance was used to compare unpaired data between three or more groups. Unadjusted two-tailed *P* values <0.05 were considered statistically significant. Kaplan-Meier survival curves were created, and the log-rank test was used to compare survival among the different groups.

*All supplementary materials are available online at [www.molmed.org](http://www.molmed.org).*

## RESULTS

### Dose-Response Effects of Radiation

The mice showed dose-response effects when irradiated with two different doses of radiation (20 or 14 Gy). XRT induced a dose-dependent reduction in the contractile reserve at 72 h and 4 months, measured as the percentage change in LVEF after isoproterenol injection (Figure 1). XRT also induced a dose-dependent decrease in the LVEF (Figure 1) and increase in LVEDP (Figure 1). The significant increase in LVEDP with XRT 20 Gy was not associated with changes in LVPSP or in  $+dP/dt$  and  $-dP/dt$  (Table 1), reflecting an increase in LV stiffness or elastance, rather than impairment in active relaxation.

### Effects of IL-1 Signal Blockade on Acute Myocardial Damage

IL-1R1 KO mice, which are not responsive to IL-1, were also irradiated with the two doses of XRT (20 or 14 Gy). The impairment in contractile reserve, at 72 h after XRT, seen in the wt mice, was significantly blunted in IL-1R1 KO mice (Figures 2, 3). Treatment of irradiated wt mice with anakinra, used to simulate a therapeutic intervention, led also to a preservation of the contractile reserve 72 h after XRT (Figures 2, 3).

### Effects of IL-1 Signal Blockade on RT-Induced Cardiomyopathy

IL-1R1 KO mice had no significant reduction in baseline LVEF and a milder reduction in contractile reserve after XRT

(Figure 4). Treatment with anakinra for 7 d preserved LVEF and contractile reserve at 3 d, but the benefits were no longer seen at 4 months (Figure 4).

No significant differences were observed in the LV diameters comparing the different groups of mice (Supplementary Table S1).

### Effects of IL-1 Signal Blockade on LV Hemodynamic

A significant increase in LVEDP after XRT 20 Gy was also seen in the IL-1R1 KO mice and in wt mice treated with anakinra (Figure 5). These results highlight the dissociation between LV contractile function and stiffness. Supplementary Figure S1 and Table 2 show data regarding hemodynamic measurements in the XRT 14 Gy group.

### Effects of IL-1 Signal Blockade on Fibrosis and Capillary Density

The reparative fibrosis after injury may be responsible for increased cardiac stiffness (24). Quantification of fibrosis in the myocardium and pericardium revealed an increase in collagen deposition after XRT 20 Gy in the wt mice, as well as in IL-1R1 KO mice or in the wt mice treated with anakinra (Figure 6). This scenario supports the dissociation between LV contractile function and fibrosis causing increased stiffness. XRT 14 Gy induced a milder increase in fibrosis (Supplementary Figure S2).

Radiation induced damage to the microvasculature reflected in a mild reduction in capillary density in the wt 20 Gy-treated mice; therefore, no significant improvements were expected in the IL-1R1 KO mice (Supplementary Figure S3).

### Effects of IL-1 Signal Blockade on Survival

A marked increase in mortality was seen at 4 months after XRT 20 Gy in both wt and IL-1R1 KO mice (Figure 7). Treatment of wt mice with anakinra had no significant effect on survival after XRT 20 Gy, with a survival curve superimposed to that of the IL-1R1 KO mice.

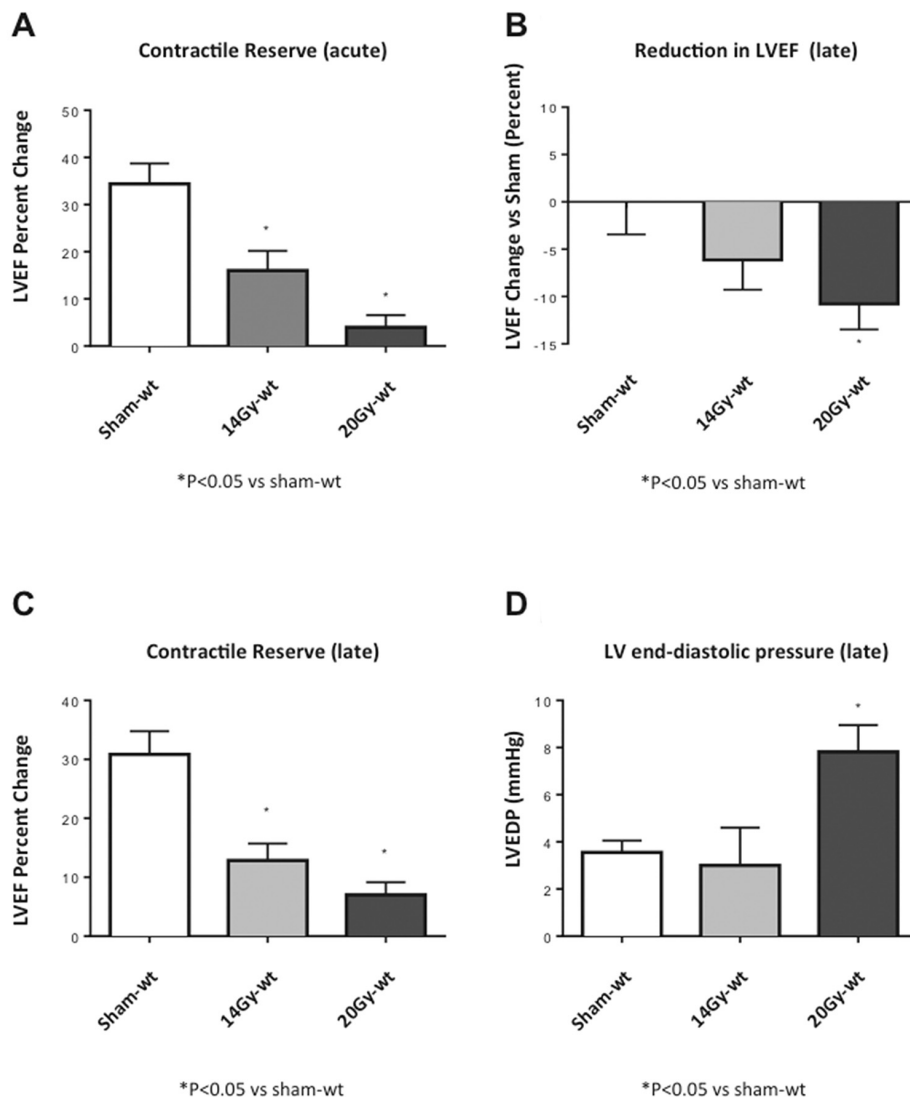


**Figure 1.** Dose-response effects of XRT. Mice receiving two different doses of radiation in a single treatment (20 or 14 Gy) showed a dose-response effect at echocardiography and with hemodynamic measurements. (A) Contractile reserve assessed at 72 h after receiving XRT treatments (20 or 14 Gy) as a change in left ventricular ejection fraction (LVEF) measured at rest and 3 min after isoproterenol injection. (B) LVEF at rest, measured 4 months after XRT and expressed as percentage reduction versus sham. (C, D) Contractile reserve assessed and LVEDP measured at 4 months after XRT.

All mice irradiated with 14 Gy (100% of wt and IL-1R1 KO) survived to 6 months, as did all the sham-irradiated mice.

## DISCUSSION

XRT-induced cardiomyopathy is a heterogeneous disease characterized by a dose-dependent progressive impairment

in contractile reserve and a decrease in LV systolic function, an increase cardiac stiffness due to myocardial and pericardial fibrosis, and premature death (4,24–26). The mechanisms involved in the progression of systolic dysfunction and fibrosis are incompletely understood. The results of this study show that IL-1 amplifies myocardial injury after

XRT and mediates the reduction of contractile reserve and LV systolic function. Genetic and pharmacological blockade of IL-1, indeed, limited the degree of injury, measured as preserved contractile reserve and LV systolic function up to 4 months after XRT. IL-1 blockade, however, did not protect from the development of myocardial and pericardial fibrosis and premature death associated with high dose (20 Gy) XRT, thus showing that IL-1 mediates some but not all the processes associated with XRT-induced cardiomyopathy.

IL-1 is a key inflammatory mediator involved in the amplification of the tissue inflammatory response (11–13). IL-1 $\beta$  is synthesized as an inactive precursor (pro-IL-1 $\beta$ ) that is cleaved by caspase-1 following formation of the inflammasome consequent to tissue injury, as following XRT (11–13,27,28). The activation of the inflammasome pathway may be due to the production of reactive oxygen species after exposure to ionizing radiation or to the production or release of damage-associated molecular patterns by irradiated cells (27–30). Activation of the inflammasome then leads to IL-1 $\beta$  processing and release, and inflammatory cell death, leading to amplification of the inflammatory response and injury (31). Recent studies have highlighted the involvement of IL-1 signaling in heart disease (13). IL-1 has been shown to induce impairment in  $\beta$ -adrenergic responsiveness and contractility, both *in vitro* and *in vivo* (16,32). Single or repeated injections of recombinant murine IL-1 $\beta$  induce systolic dysfunction and impaired contractile reserve in absence of structural changes (16,33).

Injury to the heart during irradiation leads to an inflammatory response (6,34). We hypothesized that IL-1 mediated the inflammatory response and the progression of the cardiomyopathy. Accordingly, in our mouse model, XRT induced myocardial injury and impaired the contractile reserve, measured as response to  $\beta$ -adrenergic receptor stimulation, and the resting LV systolic function in the wt mice, yet this effect was not seen in the

**Table 1.** Hemodynamic parameters.

Group <sup>a</sup>	LVPSF (mmHg)	LVEDP (mmHg)	+dP/dt (mmHg/s)	-dP/dt (mmHg/s)
Sham-wt	66.3 ± 3.7	3.6 ± 0.5	+3,708 ± 205	-3,375 ± 279
Sham-IL-1R1 KO	57.3 ± 2.3	2.4 ± 0.4	+2,975 ± 210	-2,900 ± 247
20Gy-wt	67.5 ± 2.2	7.8 ± 1.0 <sup>b</sup>	+3,450 ± 319	-3,225 ± 248
20Gy-IL-1R1 KO	63.6 ± 2.6	8.1 ± 4.2 <sup>c</sup>	+3,528 ± 985	-2,500 ± 658
20Gy-wt+anakinra	72.2 ± 3.1	9.1 ± 2.7 <sup>b</sup>	+3,650 ± 650	-2,750 ± 450

<sup>a</sup>See Experimental Groups in Materials and Methods for information on the groups.

<sup>b</sup>P < 0.05 versus sham-wt.

<sup>c</sup>P = 0.05 versus sham-IL-1R1 KO.

IL-1R1 KO mice, and it could be prevented by pharmacological IL-1 blockade with anakinra.

The genetic deletion of the IL-1R1 and the treatment with anakinra should produce the same effect. The differences between IL-1R1 KO mice and anakinra-treated mice may be related to the following: (a) the small sample size; (b) a short period of pharmacological intervention with anakinra versus the permanent deletion of the IL-1R1 gene (that is, 7 d of treatment lead to cardioprotection in the acute phase that was lost 4 months after); (c) binding of anakinra to IL-1R1,

a decoy receptor that is not expected to affect outcomes but may sequester IL-1Ra; (d) intracellular effects of IL-1Ra independent of the IL-1R1 (35); and (e) incomplete deletion of the IL-1R1 expression in some strains of IL-1R1 KO mice due to the expression of a shortened gene product in lung vasculature, as previously reported (36).

Anakinra treatment for 7 d was chosen after considering prior results in the mouse model of AMI. In this model, we found that time of treatment was sufficient to reduce adverse remodeling in the long term without rebound effects due to

interruption of the treatment (37,38). However, considering that anakinra preserved the contractile reserve at 3 d but not at 4 months, we speculate that a longer treatment with anakinra may be needed.

Although there was a reduction in the LV systolic function at rest in the irradiated wt mice, we did not observe a decrease in +dP/dt. The difference may reside in the different loading dependence on the two techniques: invasively measured +dP/dt is more preload dependent and the LVEF is more afterload dependent.

IL-1 blockade was not sufficient to prevent the increase in myocardial and pericardial fibrosis or to improve survival after high-dose XRT. In models of acute myocardial infarction (AMI), genetic or pharmacological inhibition of IL-1 reduces LV dysfunction, limits the adverse remodeling process and has no effects on myocardial fibrosis, yet reduces mortality (18,20,39–42). There appear to be similarities and differences in the role of IL-1 in the ischemic and XRT-induced cardiomyopathy. We suspect that the discrepancies between ischemic injury and XRT-induced cardiomyopathy may be related to differences in their respective pathophysiology. The cause of death in mice with AMI is mostly due to cardiac rupture or pump failure occurring early during the course (43). The effects of focused irradiation of the heart in female mice using the SARRP irradiator are overall comparable to those previously reported by our group using a clinical radiation machine with a broader beam shielding the mice with lead and leaving only the chest exposed to the radiations (4). The cause of death in mice after XRT is less clear. Death occurs late in the course and is not associated with cardiac rupture or with a severe reduction in systolic function (4). Consequently, such death may be cardiac because of an arrhythmic cause or non-cardiac-associated because of injury to other organs such as the lungs or esophagus. The injury from XRT originates from the epicardial surface, and these mice experience injury to the

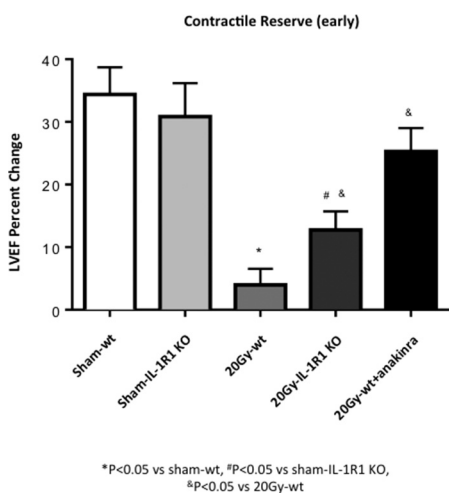


**Figure 2.** IL-1 blockade prevents reduction in contractile reserve 72 h after 20-Gy XRT. Contractile reserve was assessed 72 h after receiving 20-Gy XRT treatment as a change in LVEF measured at rest and 3 min after isoproterenol injection.

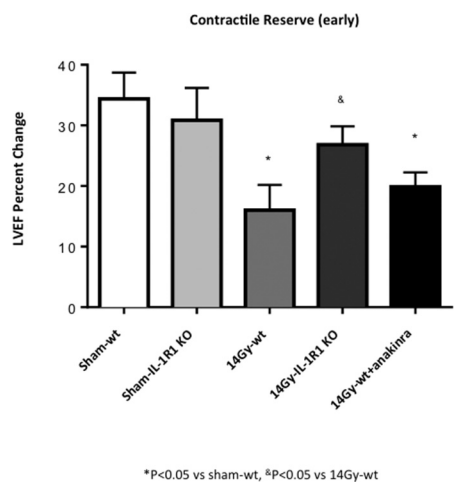


**Figure 3.** Genetic deletion of IL-1R1 prevents reduction in contractile reserve 72 h after 14-Gy XRT. Contractile reserve, assessed as a change in LVEF measured at rest and 3 min after isoproterenol injection was measured at 72 h in mice after receiving a 14-Gy single radiation dose.

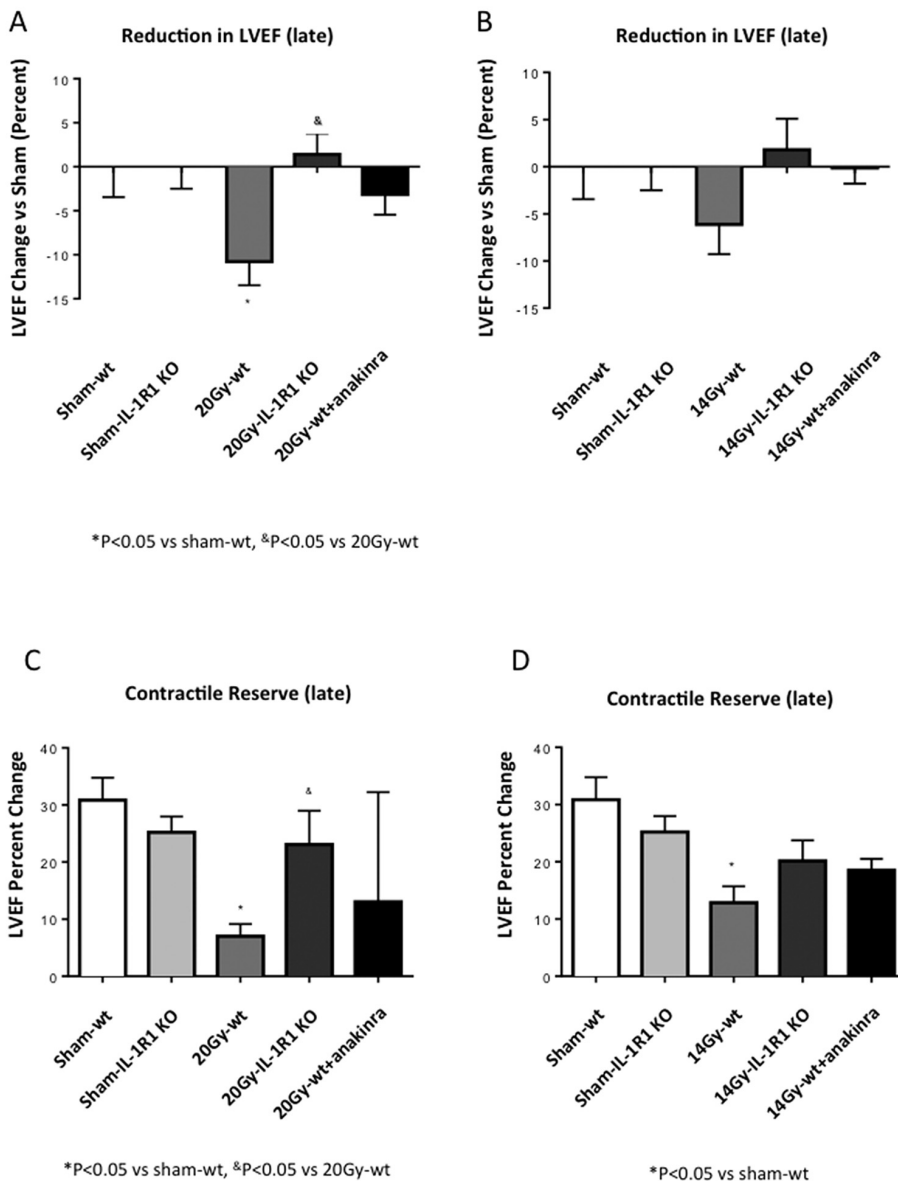


**Figure 4.** IL-1 blockade prevents XRT-induced cardiomyopathy. Four months after XRT (14 or 20 Gy), the mice underwent echocardiography to measure LVEF at rest and 3 min after  $\beta$ -adrenergic stimulation (contractile reserve). (A, B) LVEF at rest measured 4 months after XRT (20 or 14 Gy, respectively) expressed as percentage reduction versus sham. (C, D) Contractile reserve measured at 4 months after XRT (20 and 14 Gy, respectively).

heart in a distance-dependent manner; as such, it is not surprising that the most evident effect is the pericardial fibrosis in this model (6), whereas in the AMI model, the ischemic injury initiates from the endocardium. Therefore, subendocardial and transmural myocardial fibrosis is seen, but epicardial or pericardial fi-

brosis occurs rarely and only when the injury is transmural (44). The marked increase in LV end diastolic pressure in the absence of changes in  $-dP/dt$  suggests increased cardiac stiffness (reduced compliance), as with a mechanical obstacle to filling that is consistent with pericardial constriction or myocardial restric-

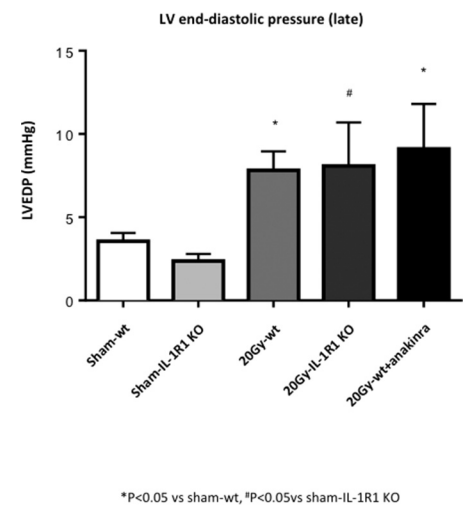


**Figure 5.** LV hemodynamic measurements. Measure of LVEDP in the groups of mice treated with 20-Gy XRT.

tion due to epicardial fibrosis (45). In patients, the cardiomyopathy associated with XRT indeed presents more like a restrictive cardiomyopathy or constrictive pericarditis (with small LV volumes, rather preserved LVEF, and markedly impaired diastolic function) than with dilated cardiomyopathy with systolic dysfunction (3).

Therefore, the mechanisms leading to myocardial and pericardial fibrosis remain unclear. The inflammatory response after radiation injury can have multiple components with a systemic “cardiodepressant” effect distinct from the fibrotic effect. We cannot exclude that the fibrotic effects could be mediated by another product of the inflammasome IL-18 (12). IL-18 is a member of the IL-1 family of cytokines and is constitutively expressed in several cell types, but it increases during inflammation, cellular stress and tissue injury (46,47). IL-18, by binding to its receptor (IL-18R), activates downstream signals that are common to the IL-1 and TLR pathways; however, the activation of the IL-18R and IL-1R1 receptors has different effects (12,46,48,49). Daily injections of IL-18 induce myocardial fibrosis in the mouse (50,51). As a product of the

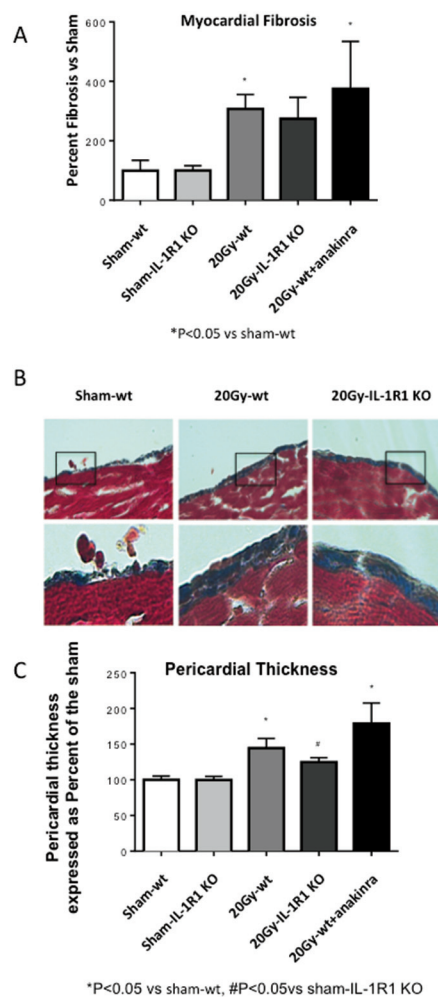


**Figure 6.** IL-1 blockade had no effects on myocardial and pericardial fibrosis. Masson’s trichrome was used to assess the total amount of interstitial collagen and the pericardial fibrosis at 4 months (20 Gy) after XRT. (A) Quantification of the myocardial interstitial fibrosis in wt mice, anakinra-treated mice and IL-1R1 KO mice. (B) Representative images of the pericardial thickness in sham and wt or IL-1R1 KO mice. (C) Quantification of the pericardial thickness in the groups of sham and 20 Gy irradiated mice. Anakinra-treated groups were compared with the sham-wt group.

inflammasome, IL-18 may therefore have a complementary effect with IL-1 on the heart in mediating XRT-induced cardiomyopathy. Further studies are needed to evaluate the effect of IL-18

blockade or inhibitors of the inflammasome in XRT-induced cardiomyopathy.

Despite the fact that IL-1 blockade failed to rescue the mice from cardiac fibrosis and premature death due to high-dose radiation (20 Gy), IL-1 blockade (genetic or pharmacologic) limited acute cardiac injury and preserved cardiac contractile function in mice. This result was particularly evident in mice with less injury to the heart due to a lower radiation dose (14 Gy). With improvements in XRT treatment planning (for example, intensity modulated therapy), injury to the heart is less common and is in less severe forms. Acute or constrictive pericarditis commonly seen in the early days of radiotherapy is now rarely seen (3). Nonetheless, the excess incidence of heart failure in patients who have received chest irradiation persists to current times and is only in part explained by accelerated coronary atherosclerosis (3). Chronic inflammation, measured by inflammatory markers, such as the C-reactive protein, is considered a risk factor for cardiovascular diseases, and several studies showed an association between radiation and chronic inflammation (52–54). Mice treated with XRT 14 or 20 Gy experienced a significant reduction in contractile reserve as early as 3 d after XRT, which was progressive over time. An impairment in contractile reserve correlates with exercise intolerance and symptoms of heart failure (16).

The finding that IL-1 mediates the reduction in contractile reserve observed with XRT-induced cardiomyopathy suggests that IL-1–targeted strategies may be useful in limiting myocardial injury acutely and potentially prevent late onset of heart failure. Impaired exercise tolerance/fatigue is the most common symptom in patients with systolic and diastolic heart failure, and a recent study has shown a significant improvement in peak aerobic exercise capacity reflecting an improved contractile reserve is evident after a short course of treatment with IL-1 blockers (16,55). Reduced exercise capacities has been associated with abnormal heart rate recovery in cancer

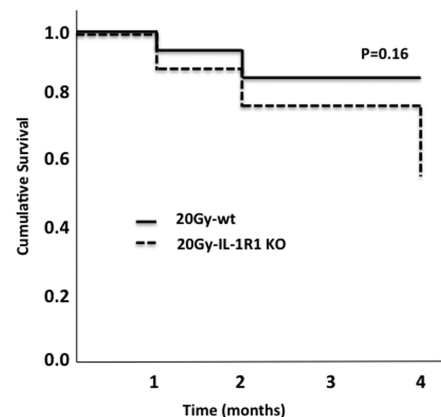


**Figure 7.** Survival curve. Kaplan-Meier curves were used to evaluate the survival rate in wt and IL-1R1 KO mice 4 months after receiving XRT treatment.

patients 20 years after thoracic radiation treatment (56). Furthermore, inflammatory markers correlate with fatigue during radiation therapy in patients with cancer (57). Whether IL-1–targeted strategies will be tolerated in patients receiving irradiation for cancer or whether such strategies will interfere with the cancer-killing properties of the irradiation is unknown and will require further study. Of interest, several studies are exploring IL-1–targeted strategies as cancer-treating strategies, and as such, IL-1 blockade may prove to serve a dual function of cardiac protection and cancer treatment (58–60).

However, the study reported herein is not free of limitations. (a) The response of the healthy mice to XRT injury may differ from that seen in mice with cancer, and may differ even more from that in patients with cancer. As such, translation should be considered with caution. (b) Although the presence of impaired contractile reserve preceding LV systolic dysfunction and the cardiac fibrosis resemble many aspects of the clinical syndrome of XRT-induced cardiomyopathy in patients, other aspects (that is, accelerated atherosclerosis) are not explored in this model. (c) While we show clear evidence of enhanced IL-1 activity mostly through evidence of benefit from genetic

and pharmacological IL-1 blockade, we do not provide direct measurements of IL-1 $\beta$  or IL-1 $\alpha$  in the heart of irradiated mice, since it is not uncommon to have undetectable tissue or plasma levels despite clear evidence of increased IL-1 activity. (d) We based our conclusions on the findings of “loss of function” strategies (IL-1R1 KO and antagonist) and have not used a “gain of function” approach in which IL-1 activity is enhanced, such as the IL-1 receptor antagonist (IL-1Ra) KO (20). (e) By using IL-1R1 KO mice or anakinra as IL-1–blocking strategies, we were unable to distinguish between the specific effects of IL-1 $\beta$  or IL-1 $\alpha$  on the observed phenotype. (f) IL-1 affects contractility through multiple and nonexclusive mechanisms affecting intracellular calcium and calcium-sensitivity (13), and we have not explored which mechanism is specifically involved in radiation-induced cardiomyopathy. (g) The blockade of IL-1 signaling did not affect the survival rate. (h) We limited our analysis to the heart and did not include other organs in which the role of IL-1 may be different (61).

## CONCLUSION

IL-1 blockade preserves LV contractile reserve and systolic function after XRT (14–20 Gy) in the mouse. However, IL-1 blockade fails to rescue the mouse from severe myocardial and pericardial fibrosis and premature death in the mouse undergoing high-dose XRT (20 Gy). These data indicate that IL-1 mediates some but not all the processes involved in the progression of XRT-induced cardiomyopathy. As such, we may foresee IL-1 blockade to improve some aspects of the disease in cancer patients undergoing radiation therapy (that is, exercise intolerance, fatigue) but not others (that is, constrictive pericarditis in patients treated with high doses of XRT) (56,57). The timing of IL-1 blockade in relation to cancer treatment needs to be clarified before one can design a clinical trial in this area, and additional studies on the pathogenesis of XRT-induced cardiomyopathy are needed.

## ACKNOWLEDGMENTS

The study was funded by a Virginia Commonwealth University Massey Cancer Pilot Research Study Award to A Abbate, by an explorative/development grant by the National Institute of Research to A Abbate and DA Gewirtz (ID 1R21CA171974-01A1), and by the American Heart Association with a Postdoctoral Fellowship grant to E Mezzaroma (ID 12POST11940005). DA Gewirtz was supported by an Institutional Research Grant (IRG-14-192-40) from the American Cancer Society. RB Mikkelsen was funded by National Institutes of Health grant 5U19AI10910361, University of Rochester Center for Medical Countermeasures against Radiation.

## DISCLOSURE

The authors declare that they have no competing interests as defined by *Molecular Medicine*, or other interests that might be perceived to influence the results and discussion reported in this paper.

## REFERENCES

- Lipshultz SE, et al. (2013) Long-term cardiovascular toxicity in children, adolescents, and young adults who receive cancer therapy: pathophysiology, course, monitoring, management, prevention, and research directions: a scientific statement from the American Heart Association. *Circulation*. 128:1927–95.
- Jaworski C, Mariani JA, Wheeler G, Kaye DM. (2013) Cardiac complications of thoracic irradiation. *J. Am. Coll. Cardiol.* 61:2319–28.
- Lipshultz SE, Adams MJ. (2010) Cardiotoxicity after childhood cancer: beginning with the end in mind. *J. Clin. Oncol.* 28:1276–81.
- Mezzaroma E, et al. (2012) A mouse model of radiation-induced cardiomyopathy. *Int. J. Cardiol.* 156:231–3.
- Monceau V, et al. (2010) Modulation of the Rho/ROCK pathway in heart and lung after thorax irradiation reveals targets to improve normal tissue toxicity. *Curr. Drug Target.* 11:1395–404.
- Seemann I, et al. (2012) Irradiation induced modest changes in murine cardiac function despite progressive structural damage to the myocardium and microvasculature. *Radiother. Oncol.* 103:143–50.
- Van Der Meeren A, Squiban C, Gourmelon P, LaFont H, Gaugler MH. (1999) Differential regulation by IL-4 and IL-10 of radiation-induced IL-6 and IL-8 production and ICAM-1 expression by human endothelial cells. *Cytokine.* 11:831–8.
- O'Brien-Ladner A, Nelson ME, Kimler BF, Wes-

selius LJ. (1993) Release of interleukin-1 by human alveolar macrophages after in vitro irradiation. *Radiat. Res.* 136:37–41.

- Tabata C, et al. (2006) All-trans retinoic acid modulates radiation-induced proliferation of lung fibroblasts via IL-6/IL-6R system. *Am. J. Physiol. Lung Cell Mol. Physiol.* 290:L597–606.
- Bentzen SM. (2006) Preventing or reducing late side effects of radiation therapy: radiobiology meets molecular pathology. *Nat. Rev. Cancer.* 6:702–13.
- Dinarello CA. (2011) Interleukin-1 in the pathogenesis and treatment of inflammatory diseases. *Blood.* 117:3720–32.
- Toldo S, et al. (2015) The inflammasome in myocardial injury and cardiac remodeling. *Antioxid. Redox. Signal.* 22:1146–61.
- Van Tassel BW, Toldo S, Mezzaroma E, Abbate A. (2013) Targeting interleukin-1 in heart disease. *Circulation.* 128:1910–23.
- Rubin P, Johnston CJ, Williams JP, McDonald S, Finkelstein JN. (1995) A perpetual cascade of cytokines postirradiation leads to pulmonary fibrosis. *Int. J. Radiat. Oncol. Biol. Phys.* 33:99–109.
- Krüse JJ, et al. (2001) Structural changes in the auricles of the rat heart after local ionizing irradiation. *Radiother. Oncol.* 58:303–11.
- Van Tassel BW, et al. (2012) Enhanced interleukin-1 activity contributes to exercise intolerance in patients with systolic heart failure. *PLoS One.* 7:e33438.
- Toldo S, et al. (2014) Interleukin-18 mediates interleukin-1-induced cardiac dysfunction. *Am. J. Physiol. Heart Circ. Physiol.* 306:H1205–31.
- Abbate A, et al. (2008) Anakinra, a recombinant human interleukin-1 receptor antagonist, inhibits apoptosis in experimental acute myocardial infarction. *Circulation.* 117:2670–83.
- Zhu J, et al. (2010) Recombinant human interleukin-1 receptor antagonist protects mice against acute doxorubicin-induced cardiotoxicity. *Eur. J. Pharmacol.* 643:247–53.
- Abbate A, et al. (2011) Alterations in the interleukin-1/interleukin-1 receptor antagonist balance modulate cardiac remodeling following myocardial infarction in the mouse. *PLoS One.* 6:e27923.
- Committee for the Update of the Guide for the Care and Use of Laboratory Animals, Institute for Laboratory Animal Research, Division on Earth and Life Studies, National Research Council of the National Academies. (2011) *Guide for the Care and Use of Laboratory Animals*. 8th edition. Washington (DC): National Academies Press.
- Schiller NB, et al. (1989) Recommendations for quantitation of the left ventricle by two-dimensional echocardiography: American Society of Echocardiography Committee on Standards, Subcommittee on Quantitation of Two-Dimensional Echocardiograms. *J. Am. Soc. Echocardiogr.* 2:358–67.
- Mezzaroma E, et al. (2011) The inflammasome promotes adverse cardiac remodeling following



- acute myocardial infarction in the mouse. *Proc. Natl. Acad. Sci. U. S. A.* 108:19725–30.
24. Kong P, Christia P, Frangogiannis NG. (2014) The pathogenesis of cardiac fibrosis. *Cell. Mol. Life Sci.* 71:549–74.
  25. Fajardo LE, Stewart JR, Cohn KE. (1968) Morphology of radiation-induced heart disease. *Arch. Pathol.* 86:512–9.
  26. Chello M, et al. (1996) Changes in the proportion of types I and III collagen in the left ventricular wall of patients with post-irradiative pericarditis. *Cardiovasc. Surg.* 4:222–6.
  27. Fu Y, et al. (2013) Resveratrol inhibits ionising irradiation-induced inflammation in MSCs by activating SIRT1 and limiting NLRP-3 inflammasome activation. *Int. J. Mol. Sci.* 14:14105–18.
  28. Stoeklein VM, et al. (2014) Radiation exposure induces inflammasome pathway activation in immune cells. *J. Immunol.* 194:1178–89.
  29. Robbins ME, Zhao W. (2004) Chronic oxidative stress and radiation-induced late normal tissue injury: a review. *Int. J. Radiat. Biol.* 80:251–9.
  30. Schae D, Kachikwu EL, McBride WH. (2012) Cytokines in radiobiological responses: a review. *Radiat. Res.* 178:505–23.
  31. Fernandes-Alnemri T, et al. (2007) The pyroptosome: a supramolecular assembly of ASC dimers mediating inflammatory cell death via caspase-1 activation. *Cell Death Differ.* 14:1590–604.
  32. Liu SJ, Zhou W, Kennedy RH. (1999) Suppression of beta-adrenergic responsiveness of L-type Ca<sup>2+</sup> current by IL-1beta in rat ventricular myocytes. *Am. J. Physiol.* 276:H141–8.
  33. Van Tassell BW, et al. (2013) Interleukin-1β induces a reversible cardiomyopathy in the mouse. *Inflamm Res.* 62:637–40.
  34. Schultz-Hector S, Trott KR. (2007) Radiation-induced cardiovascular diseases: is the epidemiologic evidence compatible with the radiobiologic data? *Int. J. Radiat. Oncol. Biol. Phys.* 67:10–8.
  35. Vecile E, et al. (2013) Intracellular function of interleukin-1 receptor antagonist in ischemic cardiomyocytes. *PLoS One.* 8:e53265.
  36. Lawrie A, et al. (2011) Paigen diet-fed apolipoprotein E knockout mice develop severe pulmonary hypertension in an interleukin-1-dependent manner. *Am. J. Pathol.* 179:1693–705.
  37. Salloum FN, et al. (2009) Anakinra in experimental acute myocardial infarction: does dosage or duration of treatment matter? *Cardiovasc. Drugs Ther.* 23:129–35.
  38. Abbate A, Dinarello CA. (2015) Anti-inflammatory therapies in acute coronary syndromes: is IL-1 blockade a solution? *Eur. Heart J.* 36:337–9.
  39. Bujak M, et al. (2008) Interleukin-1 receptor type I signaling critically regulates infarct healing and cardiac remodeling. *Am. J. Pathol.* 173:57–67.
  40. Abbate A, et al. (2010) Interleukin-1beta modulation using a genetically engineered antibody prevents adverse cardiac remodeling following acute myocardial infarction in the mouse. *Eur. J. Heart Fail.* 12:319–22.
  41. Van Tassell BW, et al. (2010) Interleukin-1 trap attenuates cardiac remodeling after experimental acute myocardial infarction in mice. *J. Cardiovasc. Pharmacol.* 55:117–22.
  42. Toldo S, et al. (2013) Interleukin-1β blockade improves cardiac remodelling after myocardial infarction without interrupting the inflammasome in the mouse. *Exp. Physiol.* 98:734–45.
  43. Gao XM, Dart AM, Dewar E, Jennings G, Du XJ. (2000) Serial echocardiographic assessment of left ventricular dimensions and function after myocardial infarction in mice. *Cardiovasc. Res.* 45:330–8.
  44. Reimer KA, Lowe JE, Rasmussen MM, Jennings RB. (1977) The wavefront phenomenon of ischemic cell death, I: myocardial infarct size vs duration of coronary occlusion in dogs. *Circulation.* 56:786–94.
  45. Mookadam F, Jiamsripong P, Raslan SF, Panse PM, Tajik AJ. (2011) Constrictive pericarditis and restrictive cardiomyopathy in the modern era. *Future Cardiol.* 7:471–83.
  46. Puren AJ, Fantuzzi G, Dinarello CA. (1999) Gene expression, synthesis, and secretion of interleukin 18 and interleukin 1beta are differentially regulated in human blood mononuclear cells and mouse spleen cells. *Proc. Natl. Acad. Sci. U. S. A.* 96:2256–61.
  47. Woldbaek PR, et al. (2003) Increased cardiac IL-18 mRNA, pro-IL-18 and plasma IL-18 after myocardial infarction in the mouse; a potential role in cardiac dysfunction. *Cardiovasc. Res.* 59:122–31.
  48. Lee JK, et al. (2004) Differences in signaling pathways by IL-1beta and IL-18. *Proc. Natl. Acad. Sci. U. S. A.* 101:8815–20.
  49. Stuyt RJ, et al. (2005) Interleukin-18 does not modulate the acute-phase response. *J. Endotoxin Res.* 11:85–8.
  50. Platis A, et al. (2008) The effect of daily administration of IL-18 on cardiac structure and function. *Perfusion.* 23:237–42.
  51. Yu Q, et al. (2009) IL-18 induction of osteopontin mediates cardiac fibrosis and diastolic dysfunction in mice. *Am. J. Physiol. Heart Circ. Physiol.* 297:H76–85.
  52. Neriishi K, Nakashima E, Delongchamp RR. (2001) Persistent subclinical inflammation among A-bomb survivors. *Int. J. Radiat. Biol.* 77:475–82.
  53. Hayashi T, et al. (2003) Radiation dose-dependent increases in inflammatory response markers in A-bomb survivors. *Int. J. Radiat. Biol.* 79:129–36.
  54. Lipshultz SE, et al. (2012) Cardiovascular status of childhood cancer survivors exposed and unexposed to cardiotoxic therapy. *J. Clin. Oncol.* 30:1050–7.
  55. Van Tassell BW, et al. (2014) Effects of interleukin-1 blockade with anakinra on aerobic exercise capacity in patients with heart failure and preserved ejection fraction (from the D-HART pilot study). *Am. J. Cardiol.* 113:321–7.
  56. Groarke JD, et al. (2015) Abnormal exercise response in long-term survivors of hodgkin lymphoma treated with thoracic irradiation: evidence of cardiac autonomic dysfunction and impact on outcomes. *J. Am. Coll. Cardiol.* 65:573–83.
  57. Bower JE, et al. (2009) Inflammatory biomarkers and fatigue during radiation therapy for breast and prostate cancer. *Clin. Cancer Res.* 15:5534–40.
  58. Lust JA, et al. (2009) Induction of a chronic disease state in patients with smoldering or indolent multiple myeloma by targeting interleukin 1β-induced interleukin 6 production and the myeloma proliferative component. *Mayo Clin. Proc.* 84:114–22.
  59. Anakinra or Denosumab and Everolimus in Advanced Cancer [Internet]. [study last updated 2015 Apr 7; cited 2015 Jun 11]. Available from: <https://www.clinicaltrials.gov/ct2/show/NCT01624766?term=NCT01624766&rank=1>. ClinicalTrials.gov Identifier: NCT01624766.
  60. Study Evaluating the Influence of LV5FU2 Bevacizumab Plus Anakinra Association on Metastatic Colorectal Cancer (IRAFU) [Internet]. [study last updated 2015 Mar 25; cited 2015 Jun 11]. Available from: <https://www.clinicaltrials.gov/ct2/show/study/NCT02090101?term=NCT02090101&rank=1>. ClinicalTrials.gov Identifier: NCT02090101.
  61. Toldo S, et al. (2015) Independent roles of the priming and the triggering of the NLRP3 inflammasome in the heart. *Cardiovasc. Res.* 105:203–12.

Cite this article as: Mezzaroma E, et al. (2015) Role of interleukin-1 in radiation-induced cardiomyopathy. *Mol. Med.* 21:210–8.